

## A LIGHT ECHO FROM TYPE Ia SN 1995E?

JASON L. QUINN AND PETER M. GARNAVICH

Physics Department, University of Notre Dame, IN 45556; jquinn@nd.edu, pgarnavi@miranda.phys.nd.edu

WEIDONG LI

Department of Astronomy, University of California, Berkeley, CA 94720-3411; weidong@astro.berkeley.edu

NINO PANAGIA AND ADAM RIESS

Space Telescope Science Institute, 3700 San Martin Drive, Baltimore, MD 21218; panagia@stsci.edu, ariess@stsci.edu

BRIAN P. SCHMIDT

Mount Stromlo and Siding Spring Observatory, Private Bag, Weston Creek P.O., Canberra,  
 ACT 2601, Australia; brian@mso.anu.edu.au

AND

MASSIMO DELLA VALLE

Osservatorio Astrofisico di Arcetri, Largo Enrico Fermi 5, 50125-Firenze, Italy; massimo@arcetri.astro.it

Received 2006 June 13; accepted 2006 July 17

### ABSTRACT

We identify a light echo candidate from *Hubble Space Telescope* (*HST*) imaging of NGC 2441, the host galaxy of the Type Ia supernova 1995E. From the echo's angular size and the estimated distance to the host galaxy, we find a distance of  $207 \pm 35$  pc between the dust and the site of the supernova. If confirmed, this echo brings the total number of observed nonhistorical Type Ia light echoes to three—the others being SN 1991T and SN 1998bu—suggesting that they are not uncommon. We compare the properties of the known Type Ia supernova echoes and test models of light echoes developed by Patat and coworkers. *HST* photometry of the SN 1991T echo shows a fading, which is consistent with scattering by dust distributed in a sphere or shell around the supernova. Light echoes have the potential to answer questions about the progenitors of Type Ia supernovae, and more effort should be made for their detection, given the importance of Type Ia supernovae to measurements of dark energy.

*Subject heading:* supernovae: individual (SN 1995E, NGC 2441)

*Online material:* color figures

### 1. INTRODUCTION

Light echoes are produced by radiation scattered by dust near or along the line of sight to an astrophysical explosion. Initially seen in Nova Per 1901 (Ritchey 1901) and then much later in Type II supernova (SN) 1987A (Crotts 1988), a flourish of light echoes has recently been observed. Spectacular examples have been detected for the peculiar star V838 Mon (Bond et al. 2003) and the so-called ancient or historical SNe in the Large Magellanic Cloud (LMC; Rest et al. 2005). Even distant gamma-ray bursts have been found to produce X-ray echoes by scattering off Galactic dust (Vaughan et al. 2004). Other events include the Type II SNe 1993J (Sugerman & Crotts 2002), 1999ev (Maund & Smartt 2005), and 2003gd (Sugerman 2005; Van Dyk et al. 2006), and two recent (i.e., nonhistorical) Type Ia SNe: 1991T (Schmidt et al. 1994) and 1998bu (Cappellaro et al. 2000; Garnavich et al. 2001). This paper reports a candidate for a third Type Ia SN light echo.

Type Ia SNe, in particular, are important as distance indicators for cosmology, but their reliability could be improved by a better understanding of the explosion mechanism and progenitors; thus, it is intriguing to consider using light echoes to probe their environments. Important clues to the distribution and properties of the dust in their vicinity may be found by studying the brightness and geometry of SN Ia light echoes. The distance between the dusty region and light source is readily calculable with a few simplifying assumptions about the dust distribution (Couderc 1939; Sugerman 2003). Further information such as polarization mea-

surements could even provide independent distance measurements between the observer and the explosive event (Sparks et al. 1999). A statistical estimate of the distribution of SN Ia relative to the structures in spiral galaxies will become possible as the sample size grows.

The peak luminosity of a SN Ia is known to correlate with host galaxy morphology (Hamuy et al. 1996) and star formation history (Gallagher et al. 2005) so that the intrinsically faintest events occur in E/S0 galaxies and hosts with low current star formation rate. The progenitors of the brighter SNe Ia in spirals appear to be associated with dusty regions and come from a young population (Mannucci et al. 2005); therefore, they have a good chance of producing a light echo. A pair of Type Ia SNe, 2002ic and 2005gj, have, in any case, recently been observed in dense circumstellar environments (Hamuy et al. 2003; Prieto et al. 2005; Aldering et al. 2006). If the mass-donating stars in SNe Ia binary progenitors are giants, then circumstellar dust may also be detectable through light echoes.

Here we present evidence of a third light echo generated from a recent SN Ia event. SN 1995E was discovered near maximum light on 1995 February 20.85 UT by A. Gabrielić (Molaro et al. 1995a). The spectral identification as Type Ia was made by Molaro et al. (1995b). A spectrum was obtained by Riess et al. (1997), and Riess et al. (1999) determined that it was discovered near maximum light, had a typical decline-rate parameter [ $\Delta m_{15}(B) = 1.06 \pm 0.05$ ], and showed more than 1 mag of visual extinction using a multicolor light-curve-shape fit. Phillips et al. (1999) found a host galaxy extinction of  $E(B - V) = 0.74 \pm 0.03$ .

## 2. THE OBSERVATIONS

*HST* Supernova/Acceleration Probe (SNAP) program 9148 took 33 Space Telescope Imaging Spectrograph (STIS) images of the locations of old Type Ia SNe in the search for new Type Ia light echoes. The STIS field of view is  $52'' \times 52''$ , and the corrected mean plate scale of the CCD is  $0.050725 \pm 0.000008$  pixel $^{-1}$ . The images were taken in direct-imaging mode (50 CCD), in which the bandpass window is determined by the detector response alone. The STIS 50 CCD has a peak throughput percentage of 14.74% at 550 nm and falls to half the peak at about 380 and 820 nm. The data products included the images and calibration data. The image preprocessing and the removal of the majority of the cosmic-ray strikes were done by the *HST* pipeline reductions.

The STIS data set included CR-split images of SN 1991T, SN 1995E, and SN 1998bu. The image of SN 1995E in NGC 2441 (an SBc/Sc spiral according to SIMBAD<sup>1</sup>) was obtained on 2001 September 4 starting at 07:37:46 (UT), approximately 2387 days after *V*-maximum,  $\Delta T$ . The images of SN 1998bu and SN 1991T were made on 2002 January 18 at 23:47:47 (UT) and 2001 November 23 at 04:11:14.7 (UT), 1486 and 3857 days past maximum, respectively. Each of these images had exposure times of 900 s.

Two data sets (proposal ID/PI: 8242/B. Savage and 9114/R. P. Kirshner) of SN 1998bu using *HST*'s Wide Field Planetary Camera 2 (WFPC2) were also downloaded from the Multimission Archive at Space Telescope (MAST). The target was in the PC field. The earlier visit, 2000 June 19, had four 320 s CR-split images (i.e., eight images of 160 s each) in F555W, and the later visit, 2002 January 10, had four 1000 s CR-split images in F439W and four 320 s CR-split images in F555W.

## 3. ANALYSIS

A resolved source is detected in the STIS images near the position of SN 1995E in a region with an otherwise smooth background, suggesting that it may be a light echo. The source is in a spiral arm in the outer regions of the galaxy about  $22.9''$  from the galactic center. The position of the light echo candidate (see Fig. 1) was compared to the position of SN 1995E in two ways. Both methods show the resolved source coincident with the SN's position.

First, the pixel position of 22 field stars and the SN were measured from eight images obtained over four nights with the 1.2 m telescope at the Fred L. Whipple Observatory (FLWO) in 1995 March, when the SN was bright. The right ascension (R.A.) and declination (decl.) for the field stars were measured from the Digitized Sky Survey at the Space Telescope Science Institute archive<sup>2</sup> and a solution computed to map the pixel positions to the celestial coordinates. The solution resulted in an rms scatter of  $0.13''$  for the field stars and a position for SN 1995E of R.A. =  $07^{\text{h}}51^{\text{m}}56^{\text{s}}.54$ , decl. =  $73^{\circ}00'35''.10$  (J2000.0). We also measured the centroid of the core of NGC 2441 to have end figures of 54.72 and 56.44 in R.A. and decl., respectively. Using the world coordinate system in the *HST* STIS image, we measure the light echo candidate to be at R.A. =  $07^{\text{h}}51^{\text{m}}56^{\text{s}}.5$ , decl. =  $73^{\circ}00'35''.06$  (J2000.0). This is a difference of  $0.027''$  in R.A. and  $0.04''$  in decl. between the suspected light echo and the position of

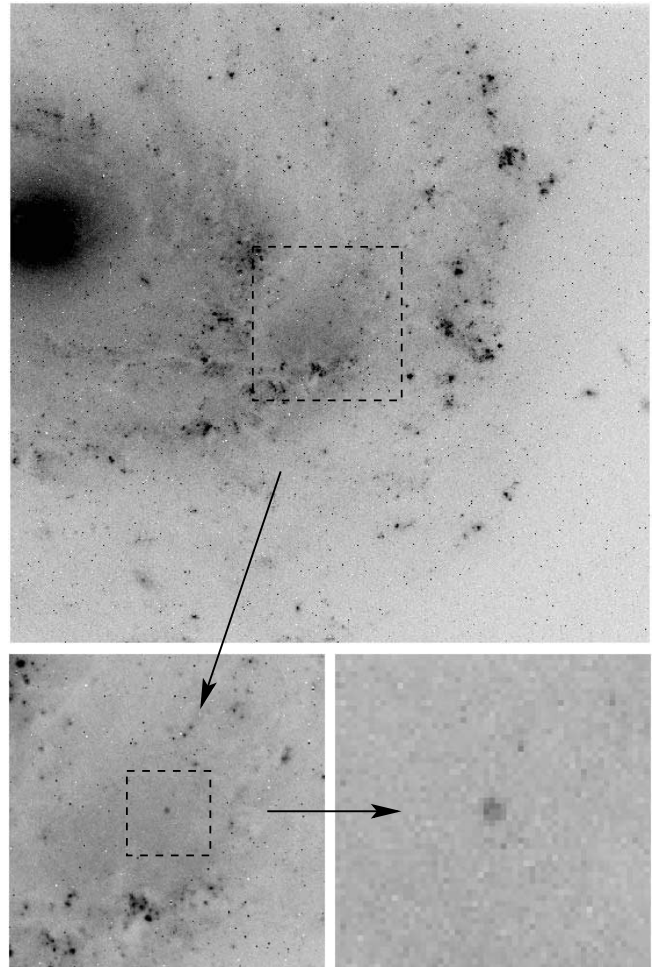


FIG. 1.—*HST* STIS close-up of SN 1995E in NGC 2441. North is to the left and east is down. The source position is R.A. =  $07^{\text{h}}51^{\text{m}}56^{\text{s}}.5$ , decl. =  $73^{\circ}00'35''.1$  (J2000.0) and  $22.9''$  from the galactic center. The image sizes are roughly  $48'' \times 48''$ ,  $12'' \times 12''$ , and  $3'' \times 3''$ .

the SN from the ground. The difference between the ground and STIS positions of the galaxy core is  $0.44''$  in R.A. and  $0.05''$  in decl.

The FLWO images were obtained in good seeing, and many features seen in the STIS image are visible in the ground-based image. The STIS images were convolved with a broad Gaussian, and the position of seven common features was measured in pixel coordinates. Using the geomap and geotrans tasks in IRAF, the FLWO image was transformed to the STIS pixel coordinates with an rms scatter of  $0.18''$ . The difference in position between the SN in the transformed FLWO image and the echo candidate in the STIS image is  $0.16''$ , which is within the error of the measurement.

### 3.1. Angular Size

The light echo candidate is resolved in the STIS image and has a full width at half-maximum (FWHM) of  $0.24 \pm 0.03''$ . The radial profile is shown in Figure 2. This diameter is small enough that the point-spread function (PSF) of the telescope contributes slightly to the image width. We can estimate the deconvolved echo radius by assuming that it is a sharp-edged disk convolved with the STIS PSF, which has a FWHM of about  $0.06''$ . This value is calculated from the intensity profile in the STIS manual. The angular size of the disk was varied until the convolved image was a good match to the observed echo width. Doing this,

<sup>1</sup> This research has made use of the SIMBAD database, operated at CDS, Strasbourg, France.

<sup>2</sup> The Digitized Sky Surveys were produced at the Space Telescope Science Institute under US Government grant NAG W-2166. The images of these surveys are based on photographic data obtained using the Oschin Schmidt Telescope on Palomar Mountain and the UK Schmidt Telescope. The plates were processed into the present compressed digital form with the permission of these institutions.

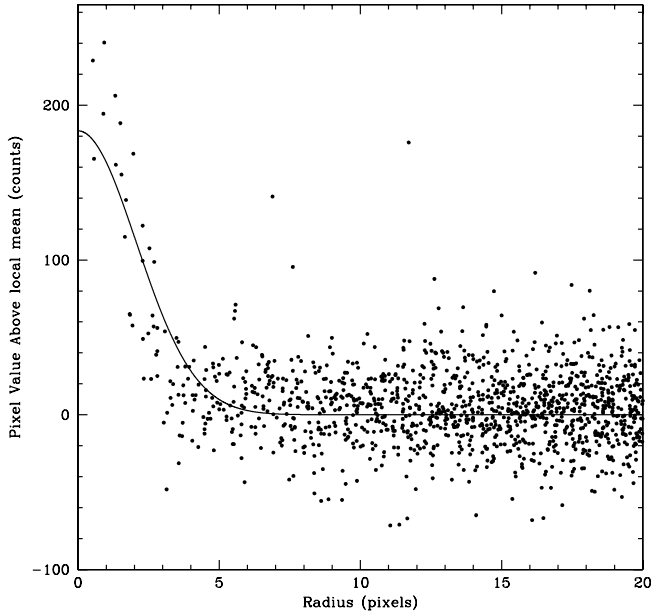


FIG. 2.—Radial profile showing, for reference, the best Gaussian fit (amplitude 183.5 and FWHM 4.87). The data are steeper than a Gaussian.

we find that the deconvolved angular radius of the echo is  $0''.12 \pm 0''.03$ , including error for the convolution process. If we assume the echo is an annulus, we do not get a good match to the observed light distribution unless the radius of the inner hole is smaller than  $0''.03$ , which is roughly half a pixel. Although one of the innermost pixels is suggestively underluminous, which could be a hint of annulus structure, the resolution of the data was too low to confirm that it exists. A convolved disk of radius  $0''.12 \pm 0''.03$  was a good match to the STIS image.

### 3.2. Dust Distance

The geometry of the dusty region causing SN 1995E's echo is an important unknown. A pioneering study by Couderc (1939) investigated light echoes for several key geometries, such as the flat dust sheet, which is one of the simplest and most important cases, and the dust cloud. An analytic treatment shows that the dust sheet produces an echo that is a circular ring containing the source, and the radius of the ring at a given time does not depend on the inclination of the sheet but rather on the distance from the SN to the dust sheet. If the sheet is perpendicular with respect to the line of sight, the source lies at the center of the ring; otherwise, the source is shifted off center. Such a shift would be small compared to the astrometric accuracy in this study. Furthermore, because the host galaxy is seen nearly face-on (cf. Fig. 1) and the dust may be associated with the disk, it is plausible that the assumption of a perpendicular plane is not as restrictive as it may at first appear and is taken hereafter. The width of the ring depends on the thickness of the dust sheet,  $\Delta R$ , and the duration of the explosive event. The thickness and duration are assumed to be small and short. Under these conditions, the distance,  $R$ , of the SN to the dust plane is given in approximation by

$$D^2 \simeq \frac{2c\Delta TR + (c\Delta T)^2}{\theta^2}, \quad (1)$$

where  $c$  is the speed of light,  $D$  is the distance to the host galaxy,  $\theta$  is the angular radius of the echo, and  $\Delta T$  is the time since maximum. This approximate formula is good to better than 0.01% for typical values compared to the exact expression. Hubble's

Law,  $D = v/H_0$ , gives the distance to the host galaxy, where  $H_0 = 70 \pm 4 \text{ km s}^{-1} \text{ Mpc}^{-1}$  (Tegmark et al. 2004). The recessional velocity of NGC 2441 is  $v = 3470 \pm 17 \text{ km s}^{-1}$  (Falco et al. 1999). This yields a distance of  $207 \pm 35 \text{ pc}$  to the dust sheet of SN 1995E. An annulus (or a solid disk, as observed in this case) instead of a thin ring would result from the breakdown of some of the simplifying assumptions of this model, such as a dust sheet that is non-negligibly thin or a finite duration of the source event.

### 3.3. Brightness

The flux,  $f_\lambda$ , and 50 CCD STIS magnitude, CL, of the image are given by the STIS Data Handbook as

$$f_\lambda = \frac{\text{counts} \times \text{PHOTFLAM}}{\text{EXPTIME}}, \quad (2)$$

$$\text{CL} = -2.5 \log f_\lambda + \text{PHOTZPT}. \quad (3)$$

The values of PHOTFLAM and PHOTZPT are given in the image headers as  $9.9509750 \times 10^{-20} \text{ ergs s}^{-1} \text{ cm}^{-2} \text{ \AA}^{-1}$  and  $-21.1 \text{ mag}$ , respectively (which corresponds to a 1 count  $\text{s}^{-1}$  magnitude of 26.41). PHOTZPT is set such that the star Vega has a Johnson  $V$ -band magnitude of zero. The STIS image yields a count rate for the echo candidate of  $4.37 \text{ DN s}^{-1}$  (3935 counts) within a 6 pixel radius aperture for a non-aperture-corrected magnitude of  $24.80 \pm 0.08$ . The error is that reported by IRAF task phot.

The target image is compact, and an aperture correction should not be much different from that of a stellar source. An aperture correction can be found using the 50 CCD energy-encircled radial profile of the STIS Instrument Handbook (Table 14.3). Linear interpolation between 5 and 10 pixels is used to find the intensity at 6 pixels. We chose 20 pixels, where the encircled energy is 99.6%, as the outer, "infinite aperture" radius. The aperture correction is  $\Delta m_{6-20} \simeq -0.093 \text{ mag}$ , so the aperture-corrected CL magnitude is  $24.71 \pm 0.13$ , which includes 0.05 mag error estimated and added just for the aperture correction.

A transformation from the CL magnitude of the 50 CCD detector with its large bandpass to a Johnson  $V$ -band magnitude is given by combining equations (1) and (2) of Rejkuba et al. (2000) and eliminating their 50 CCD – F28X50LP color variable. This yields the following equation:

$$V = \text{CL} + (0.26 \pm 0.19) \frac{(V - I) - (1.18 \pm 0.03)}{1.76 \pm 0.13} + 0.01 \pm 0.04. \quad (4)$$

The  $V$ -band magnitude thus depends on the  $V - I$  color. We have no direct estimate of the color of the SN 1995E echo, so it must be approximated. A formula connecting the unextincted color of a SN at maximum,  $(B - V)_{\text{max}}^0$ , to the color of its echo is given by equation (20) of Patat (2005) for a single-scattering plus attenuation (SSA) model. The same formula written in terms of the  $V - I$  color and rewritten in terms of the reddening instead of optical depth is

$$(V - I) \approx (V - I)_{\text{max}}^0 - 2.5 \log \frac{C_{\text{ext}}^V \omega^V \Delta t_{\text{SN}}^V}{C_{\text{ext}}^I \omega^I \Delta t_{\text{SN}}^I} + (R_V - R_I)E(B - V). \quad (5)$$

The values of the dust cross section  $C_{\text{ext}}$ , albedo  $\omega$ , and flash duration  $\Delta t_{\text{SN}}$  are shown in Table 1 for the  $B$ ,  $V$ , and  $I$  bands. The cross section and albedo were calculated using the latest synthetic

TABLE 1  
DUST PARAMETERS AND FLASH DURATIONS

Filter	$\lambda$ (Å)	$C_{\text{ext}}$ ( $10^{-22}$ cm <sup>2</sup> )	$\omega$	$\Delta t_{\text{SN}}$ (yr)
<i>B</i> .....	4300	6.59	0.65	0.0654
<i>V</i> .....	5400	4.98	0.67	0.0857
<i>I</i> .....	9000	2.36	0.64	0.102

NOTES.—The values of extinction cross section and albedo,  $C_{\text{ext}}$  and  $\omega$ , for  $R_V = 3.1$  are from Weingartner & Draine (2001) and Draine (2003). The values of the flash durations,  $\Delta t_{\text{SN}}$ , are from Patat (2005), except for  $\Delta t_{\text{SN}}^I$ , which was measured using the light curve of SN 1994D.

extinction models of Weingartner and Draine (Weingartner & Draine 2001; Draine 2003). For the flash duration, we used the *B* and *V* values reported in Patat (2005), which were based on SN 1992A and SN 1994D. We measured the *I*-band value using the light curve of SN 1994D alone (Patat et al. 1996). The *I*-band light curves of Type Ia SNe can be quite heterogeneous because of the secondary maximum, and this can affect the value of  $\Delta t_{\text{SN}}^I$ , so *cautev emptor*. The flash durations are actually weak functions of  $\Delta m_{15}(B)$ , but they were treated as constant for our SNe. Patat points out that the scattering term is small for the *B* – *V* analog of equation (5), and the echo color can be approximated by just the color of the SNe at maximum plus a term linear in the optical depth. In *V* – *I*, the scattering term is non-negligible, mostly because of the change in the ratio of the dust cross section. An even more serious concern is the effect of multiple scattering, because SN 1995E has a large optical depth along the line of sight ( $\tau_d \approx 2.1$ ). Comparison of Patat’s SSA and Monte Carlo (MC) models show that multiple scattering can play a large role even in *B* – *V* for large  $\tau_d$ .

The *V*-band magnitude of the echo can now be found from equations (4) and (5) given the extinction. But how accurate is this model? The only test case is SN 1998bu. The predicted value of its *B* – *V* color (using the *B* – *V* version of eq. [5]) compared to our measured WFPC2 color (see below) shows about a 0.2 mag difference. This is compatible with the rms scatter found by Rejkuba et al. (2000) for the color-color equations used to derive equation (4) and was assigned as the error in our *V* – *I* echo color. The *V*-band brightness of SN 1995E’s echo is  $24.57 \pm 0.18$  mag using  $R_V = 3.1$ . Using the disk previously discussed, the surface brightness is  $21.21 \pm 0.25$  mag arcsec<sup>-2</sup>. The STIS *V*-band magnitudes of SN 1991T and SN 1998bu were  $22.34 \pm 0.23$  and  $21.55 \pm 0.20$  mag, respectively.

Ratios of total-to-selective extinction of  $R_V = 3.1 \pm 0.1$  and  $R_I = 1.48$  were used above (Cardelli et al. 1989). This is to remain consistent with the lowest  $R_V$  dust and echo models, which also used  $R_V = 3.1$ . However, it is believed that Type Ia SNe have  $R_V \approx 2.55 \pm 0.3$  (Riess et al. 1996) or even as low as  $1.80 \pm 0.19$  (Elias-Rosa et al. 2006). An  $R_V$  of 2.55 would make the STIS observations for SN 1995E, SN 1991T, and SN 1998bu fainter by 0.06, 0.01, and 0.03 mag, respectively. The echo color for large optical depths is also affected by changes in  $R_V$ , but it is worth noting that the interstellar extinction law is less  $R_V$ -dependent in the *I* band than the *B* band. This mitigates some worries of the model dependencies on the dust properties, but lower  $R_V$  models would be very useful. The WFPC2 PC data set of SN 1998bu had the CR splits combined, and the resulting images for each visit and filter were averaged together (to remove the effects of sky quantization) and an instrumental magnitude was measured. The conversion of the F439W and F555W magnitudes to standard *B* and *V* magnitudes for the echo was accomplished using the method of

Holtzman et al. (1995). Their work describes the transformation of the WFPC2 flight system magnitudes with a 0.5 aperture to Johnson magnitudes. Our analysis is complicated by the extended nature of the source ( $\approx 0.83$  radius ring); it demands a larger aperture, but this will overestimate the flux. Our working solution was to use a large aperture and correct back the required 0.5 using the energy-encircled profiles in the Holtzman paper. It was necessary to use the color measured for the later visit in the calculation of the magnitude of the earlier one, since it was only imaged in F555W. We find  $V = 21.11 \pm 0.04$  on 2000 June 19, and  $B = 21.31 \pm 0.06$  and  $V = 21.24 \pm 0.05$  on 2002 January 10.

#### 4. DISCUSSION

Currently there are only two known Type Ia SNe light echoes from recent events: SN 1991T and SN 1998bu (see Table 2). All three echoes have a late-type host galaxy (i.e., >Sa). SN 1991T in NGC 4527 was a very unusual SN Ia. It showed weak spectral features and exhibited broad *B* and *V* light curves [ $\Delta m_{15}(B) = 0.94 \pm 0.05$ ]. Later it showed a more normal spectrum and decline rate; however, at about 600 days past maximum, the exponential fading slowed until the decline rate was consistent with zero, and the spectrum showed features reminiscent of a SN at maximum, an observation that was identified as the result of a light echo (Schmidt et al. 1994) caused by a dust cloud of radius 50 pc (Sparks et al. 1999). On the other hand, SN 1998bu in NGC 3368 was spectroscopically and photometrically normal except for appearing to be more reddened than usual (see Suntzeff et al. 1999) until, at around 400 days past maximum, the light curve started to deviate from the expected decline. By 700 days past maximum it had almost flattened. Cappellaro et al. (2001) attributed this behavior to a light echo caused by foreground dust roughly 100 pc away by comparing an integrated early spectrum to the late-time spectrum. Garnavich et al. (2001) discovered from *HST* WFPC2 imaging that there is not one but two echoes for this event, corresponding to dust at  $120 \pm 15$  pc and less than 10 pc away.

How does the integrated brightness of SN 1995E’s echo compare to other Type Ia light echoes? The *V*-band magnitude difference between maximum and  $\Delta T = 2387$  days ( $\sim 6.5$  yr) past maximum for SN 1995E was  $8.48 \pm 0.18$  mag. The brightness differences for SN 1991T and SN 1998bu for the same time past maximum, as can be estimated from Figure 3, are  $10.37 \pm 0.23$  and  $9.54 \pm 0.20$  mag, respectively. The data clearly indicate that the light curve of SN 1991T is declining nearly linearly in magnitude at a rate of about  $0.114$  mag yr<sup>-1</sup>. The light curve of SN 1998bu is more difficult to interpret because of the two echoes, and the baseline for the observations after the break from the normal exponential-like decline is shorter. Linear regression

TABLE 2  
TYPE Ia LIGHT ECHOES

Event	JD ( $V_{\text{max}}$ )	$V_{\text{max}}$ (mag)	$\Delta m_{15}(B)$	Host
SN 1991T.....	2,448,378.3 <sup>a</sup>	$11.51 \pm 0.02^a$	$0.94 \pm 0.05^b$	NGC 4527
SN 1995E.....	2,449,776.4	$16.09 \pm 0.02^c$	$1.06 \pm 0.05^b$	NGC 2441
SN 1998bu.....	2,450,954.4 <sup>d</sup>	$11.86 \pm 0.02^d$	$1.01 \pm 0.05^b$	NGC 3368

NOTES.—The date of maximum for SN 1995E was calculated using a parabolic fit to the brightest three data points of Riess et al. (1999). Its  $V_{\text{max}}$  error was assigned for this paper.

<sup>a</sup> From Lira et al. (1998).

<sup>b</sup> From Phillips et al. (1999).

<sup>c</sup> From Riess et al. (1999).

<sup>d</sup> From Jha et al. (1999).

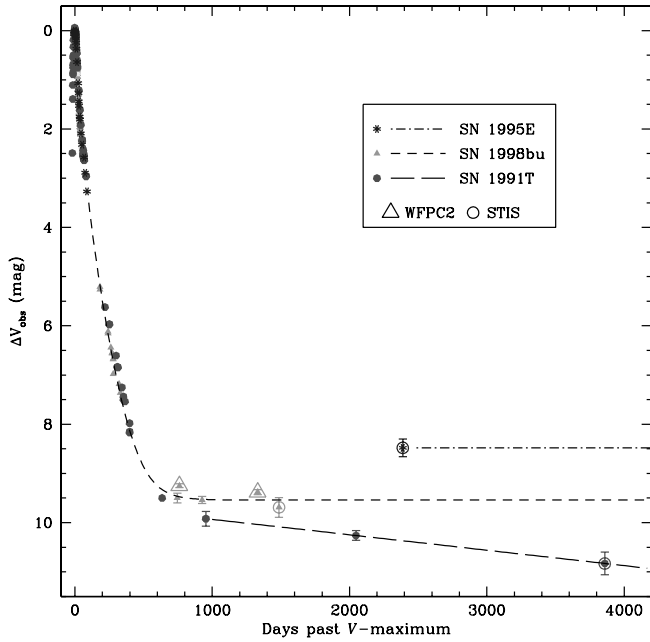


FIG. 3.—Light curves of SN 1995E, SN 1998bu, and SN 1991T, showing the decline in magnitude of the SNe from  $V_{\max}$ ,  $\Delta V_{\text{obs}}$ , as a function of time after  $V$ -maximum. Clearly the echo of SN 1991T is fading ( $\approx 0.114 \text{ mag yr}^{-1}$ ), as it perhaps is for SN 1998bu, but SN 1995E is inconclusive. The ground-based light-curve data are from Lira et al. (1998) and Schmidt et al. (1994) for SN 1991T (early- and late-time points, respectively), from Riess et al. (1999) for SN 1995E, and from Jha et al. (1999) and Suntzeff et al. (1999) for SN 1998bu. [See the electronic edition of the Journal for a color version of this figure.]

on its last points both with and without weighting indicate a slope similar to that of SN 1991T, but the error in the slope is relatively large and moreover these points are influenced by the elbow in the light curve. These things considered, the slope is consistent with zero. The models of Patat show that the luminosity of a dust sheet echo declines at a much slower rate on average than a dust cloud (roughly  $0.03\text{--}0.04$  vs.  $0.11\text{--}0.14 \text{ mag yr}^{-1}$ , depending on the optical depth); so the cloud model matches the decline rate of SN 1991T quite well. The dust sheet model for the outer echo of SN 1998bu seems strongly motivated, but the evidence suggests the possibility of a dust cloud for the inner echo. Our data do not seem inconsistent with the inner echo being produced by a dust cloud, but are too ambiguous to draw a firm conclusion from because of the short baseline of observation. It was therefore assumed to plateau, as might be expected of an echo produced by a dust sheet.

It is useful to account for the effects of extinction such that the relative brightness of each echo to the SN at maximum can be compared. Unfortunately, the line-of-sight extinction for arbitrary dust geometries does not correlate with the effective extinction of the echo (e.g., if a dust sheet has a hole directly in front of a SN, there would be less line-of-sight extinction); but to

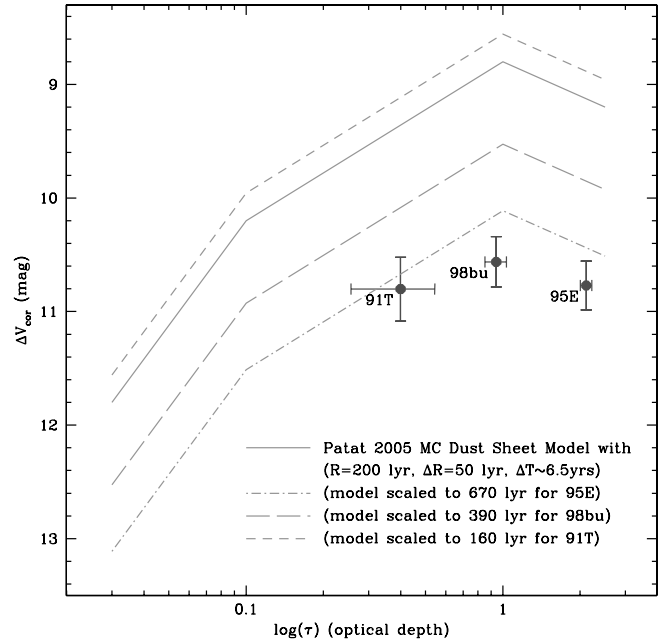


FIG. 4.—Decline in magnitude (corrected for extinction) at  $\Delta T = 2387$  days vs. the optical depth,  $\tau = A_V / (2.5 \log e)$ . The solid line data points come from the Fig. 6 Monte Carlo solutions of Patat (2005), and the dashed line points are the same model scaled via Patat’s single-scattering formula,  $4\pi d^2 F(t)/L_0 \approx 0.3\tau_d/R$ , to the dust distances of each SN (rounded to the nearest 10 lt-yr). The effect of a dust mixture change to  $R_V = 2.55$  is discussed in the text. [See the electronic edition of the Journal for a color version of this figure.]

make progress, the line-of-sight extinction was taken to be approximately equal to the effective extinction of the echo. Table 3 details how this was accomplished. The values of host galaxy extinction,  $E(B - V)$ , given in the table are those of Phillips et al. [1999; called  $E(B - V)_{\text{Avg}}$  there]. They have removed the effects of Galactic reddening using Schlegel et al. (1998) and included the  $K$ -correction to first order. Since we want the difference in the brightness of the SN to the echo, the Galactic extinction cancels. After correcting for extinction (an  $R_V$  value of 3.1 and the single-scattering approximation, for which there is no extinction along the echo light path, were used), all the observed echoes are about 10.5–11.0 mag fainter than the SN at maximum. This narrow range is somewhat striking given the diversity of the environments that could have produced the echoes. For the dust sheet approximation, the echo brightness is a fairly sensitive function of the dust distance, and closer dust results in a brighter echo. The three echoes here have a range of dust distances from roughly 200 to 700 lt-yr but show a narrow range in brightness.

The extinction-corrected echo luminosities of SN 1995E, SN 1998bu, and SN 1991T are plotted against scattering optical depth in Figure 4. Also plotted are the Monte Carlo simulations of Patat for a dust sheet of thickness 50 lt-yr ( $\sim 15.3$  pc) at 200 lt-yr

TABLE 3  
EXTINCTION-CORRECTED DECLINES

Event	$\Delta V_{\text{obs}}$ (mag)	$E(B - V)$ (mag)	$A_V$ (mag)	$\Delta V_{\text{cor}}$ (mag)
SN 1991T.....	$10.37 \pm 0.23$	$0.14 \pm 0.05$	$0.434 \pm 0.16$	$10.80 \pm 0.28$
SN 1995E.....	$8.48 \pm 0.18$	$0.74 \pm 0.03$	$2.294 \pm 0.12$	$10.77 \pm 0.22$
SN 1998bu.....	$9.54 \pm 0.20$	$0.33 \pm 0.03$	$1.023 \pm 0.10$	$10.56 \pm 0.22$

NOTES.—This table calculates the decline of the echo relative to the SN at maximum, corrected for extinction,  $\Delta V_{\text{cor}} = \Delta V_{\text{obs}} + A_V$ , where as usual  $A_V = R_V E(B - V)$ . The ratio of total-to-selective extinction was  $R_V = 3.1 \pm 0.1$ , and the extinction values of the host galaxy,  $E(B - V)$ , are those of Phillips et al. (1999). For SN 1995E and SN 1998bu, the error in  $\Delta V_{\text{obs}}$  is quite model-dependent, and these are estimates.

( $\sim 61.3$  pc; *the solid line*) and the same solution scaled to the dust distance of each SN. The luminosity of the echoes was assumed to scale inversely proportional to the dust distance via the single-scattering approximation formula,  $4\pi d^2 F(t)/L_0 \approx 0.3\tau_d/R$  (Patat 2005), for a perpendicular sheet. Here  $d$  is the distance from the observer to the SN,  $F$  is the observed integrated flux of the echo,  $L_0$  is the luminosity of the SN treating it as a flash of duration  $\Delta t_{\text{SN}}$ ,  $\tau_d$  is the optical depth, and  $R$  is the distance to the plane. The distance to SN 1995E's dust sheet as determined by this paper (Fig. 4, *dot-dashed line*) is  $207 \pm 35$  pc ( $\sim 670$  lt-yr). The predicted luminosity of SN 1995E's echo for its optical depth agrees with our data within the statistical and a reasonable model uncertainty. SN 1991T had a light echo consistent with a uniform density dust cloud of radius 50 pc ( $\sim 160$  lt-yr; Sparks et al. 1999) and is over a magnitude fainter than one would expect ( $\approx 1.1$  mag). Again, the case of SN 1998bu is more complicated because there are two echoes. The model curve shown in Figure 4 has been shifted to the 120 pc ( $\sim 390$  lt-yr) distance corresponding to the outer echo. The echo luminosity implied is also around a magnitude fainter than the model predicts ( $\approx 0.9$  mag). Both of these points appear to be underluminous for a thin-sheet model, but in both cases dust clouds, not dust sheets, are known or suspected to be involved, and very large optical depths suggesting a full MC treatment may be needed for these echoes. Changing the dust mixture to  $R_V = 2.55$  has a significant effect on the values of  $A_V$  that amounts to  $-0.12$ ,  $-0.41$ , and  $-0.18$  mag for SN 1991T, SN 1995E, and SN 1998bu, respectively. The 0.06 mag discussed earlier for the STIS  $V$ -band magnitude of SN 1995E also directly affects  $\Delta V_{\text{cor}}$ , because there is only one late-time observation. The model now closely matches SN 1995E, but the other two are still

underluminous. It will be interesting to see how the next echo discoveries compare to these.

## 5. CONCLUSIONS

We show that a resolved source resides at the position of Type Ia SN 1995E in face-on spiral NGC 2441, which is likely to be a light echo. The angular size and brightness are consistent with an echo interpretation for the source; however, further high-resolution imaging is required to test for variability in size or brightness. If it is an echo, we derive a distance of  $207 \pm 35$  pc between the scattering dust and the SN.

Comparison of the SN 1995E echo with echoes observed from SN 1991T and SN 1998bu shows a strong similarity in their integrated flux relative to the peak SN brightness, despite large variations in the dust optical depth and dust distributions. Photometry of the SN 1991T echo suggests a decline in integrated brightness, which is consistent with a cloud or shell distribution of dust around the progenitor. A new echo strengthens the case that some Type Ia SNe are near dusty environments and that a subset may be linked to a younger population. Further studies of SN Ia light echoes are needed and may provide important constraints on progenitor models and any connection between progenitors and dusty or star-forming regions.

This research has made use of the NASA/IPAC Extragalactic Database (NED), which is operated by the Jet Propulsion Laboratory, California Institute of Technology, under contract with the National Aeronautics and Space Administration.

## REFERENCES

- Aldering, G., et al. 2006, ApJ, 650, 510  
 Bond, H. E., et al. 2003, Nature, 422, 405  
 Cappellaro, E., Benetti, S., Pastorello, A., Turatto, M., Altavilla, G., & Rizzi, L. 2000, IAU Circ. 7391, 1  
 Cappellaro, E., et al. 2001, ApJ, 549, L215  
 Cardelli, J. A., Clayton, G. C., & Mathis, J. S. 1989, ApJ, 345, 245  
 Couderc, P. 1939, Ann. d'Astrophys., 2, 271  
 Crotts, A. 1988, ApJ, 333, L51  
 Draine, B. T. 2003, ApJ, 598, 1017  
 Elias-Rosa, N., et al. 2006, MNRAS, 369, 1880  
 Falco, E. E., et al. 1999, PASP, 111, 438  
 Gallagher, J. S., Garnavich, P. M., Berlind, P., Challis, P., Jha, S., & Kirshner, R. P. 2005, ApJ, 634, 210  
 Garnavich, P. M., et al. 2001, BAAS, 33, 1370  
 Hamuy, M., Phillips, M. M., Suntzeff, N. B., Schommer, R. A., Maza, J., Smith, R. C., Lira, P., & Aviles, R. 1996, AJ, 112, 2438  
 Hamuy, M., et al. 2003, Nature, 424, 651  
 Holtzman, J. A., Burrows, C. J., Casertano, S., Hester, J. J., Trauger, J. T., Watson, A. M., & Worthey, G. 1995, PASP, 107, 1065  
 Jha, S., et al. 1999, ApJS, 125, 73  
 Lira, P., et al. 1998, AJ, 115, 234  
 Mannucci, F., Della Valle, M., Panagia, N., Cappellaro, E., Cresci, G., Maiolino, R., Petrosian, A., & Turatto, M. 2005, A&A, 433, 807  
 Maund, J. R., & Smartt, S. J. 2005, MNRAS, 360, 288  
 Molaro, P., Gabrielse, A., Boehm, C., & Tescicini, G. 1995b, IAU Circ. 6137, 1  
 Molaro, P., Vladilo, G., & Walton, N. A. 1995a, IAU Circ. 6140, 3  
 Patat, F. 2005, MNRAS, 357, 1161  
 Patat, F., Benetti, S., Cappellaro, E., Danziger, I. J., Della Valle, M., Mazzali, P. A., & Turatto, M. 1996, MNRAS, 278, 111  
 Phillips, M. M., Lira, P., Suntzeff, N. B., Schommer, R. A., Hamuy, M., & Maza, J. 1999, AJ, 118, 1766  
 Prieto, J., Garnavich, P., Depoy, D., Marshall, J., Eastman, J., & Frank, S. 2005, IAU Circ. 8633, 1  
 Rejkuba, M., Minniti, D., Gregg, M. D., Zijlstra, A. A., Alonso, M. V., & Goudfrooij, P. 2000, AJ, 120, 801  
 Rest, A., et al. 2005, Nature, 438, 1132  
 Riess, A. G., Press, W. H., & Kirshner, R. P. 1996, ApJ, 473, 588  
 Riess, A. G., et al. 1997, AJ, 114, 722  
 ———. 1999, AJ, 117, 707  
 Ritchey, G. 1901, ApJ, 14, 293  
 Schlegel, D. J., Finkbeiner, D. P., & Davis, M. 1998, ApJ, 500, 525  
 Schmidt, B. P., Kirshner, R. P., Leibundgut, B., Wells, L. A., Porter, A. C., Ruiz-Lapuente, P., Challis, P., & Filippenko, A. V. 1994, ApJ, 434, L19  
 Sparks, W. B., Macchetto, F., Panagia, N., Boffi, F. R., Branch, D., Hazen, M. L., & Della Valle, M. 1999, ApJ, 523, 585  
 Sugerman, B. E. K. 2003, AJ, 126, 1939  
 ———. 2005, ApJ, 632, L17  
 Sugerman, B. E. K., & Crotts, A. P. S. 2002, ApJ, 581, L97  
 Suntzeff, N. B., et al. 1999, AJ, 117, 1175  
 Tegmark, M., et al. 2004, Phys. Rev. D, 69, 103501  
 Van Dyk, S. D., et al. 2006, PASP, 118, 351  
 Vaughan, S., et al. 2004, ApJ, 603, L5  
 Weingartner, J. C., & Draine, B. T. 2001, ApJ, 548, 296